A Compact Photochromic Occlusion Capable See-through Display with Holographic Lenses

Chun-Wei Ooi*
Trinity College Dublin

Yuichi Hiroi†
The University of Tokyo

Yuta Itoh‡
The University of Tokyo

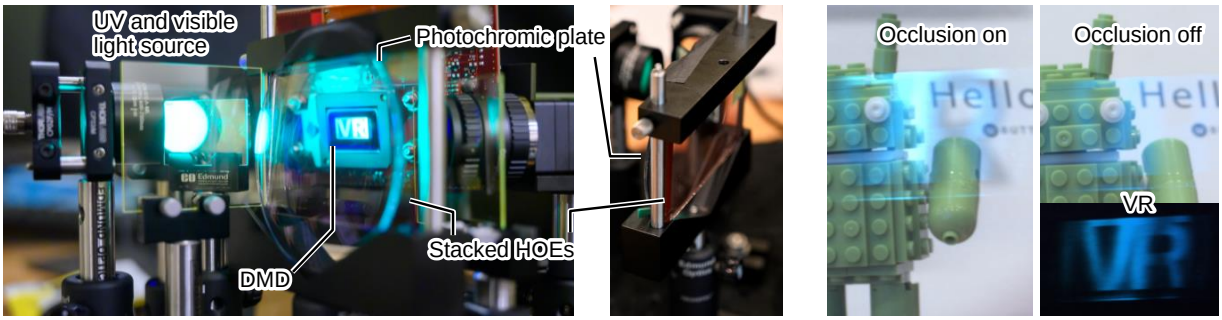

Figure 1: Our proof-of-concept system of a photochromic occlusion-capable optical OST-NED. Our main contribution is to demonstrate that integrating a stack of reflective and refractive HOLs, which interact with both UV and visible light separately, enables a compact photochromic occlusion-capable OST-NED. (a) A working prototype of the system. The light sources on the left emit UV and green light, and the DMD displays a mask image and a visible image in a time-separated manner. The stacked HOLs then split the image beams toward the photochromic plate and the viewpoint. (b) Side view of the stacked photochromic plate and the HOLs. (c) Displayed image with the photochromic occlusion mask. Note that the light color density of the occlusion mask is due to the low maximum optical density of the material used. (d) Displayed image without occlusion mask. (d, top) See-through view and (d, bottom) dark room environment. The contrast of the see-through view is decreased compared to the case with the occlusion mask.

Abstract

Occlusion is a crucial visual element in optical see-through (OST) augmented reality, however, implementing occlusion in OST displays while addressing various design trade-offs is a difficult problem. In contrast to the traditional method of using spatial light modulators (SLMs) for the occlusion mask, using photochromic materials as occlusion masks can effectively eliminate diffraction artifacts in see-through views due to the lack of electronic pixels, thus providing superior see-through image quality. However, this design requires UV illumination to activate the photochromic material, which traditionally requires multiple SLMs, resulting in a larger form factor for the system.

This paper presents a compact photochromic occlusion-capable OST design using multilayer, wavelength-dependent holographic optical lenses (HOLs). Our approach employs a single digital micromirror display (DMD) to form both the occlusion mask with UV light and a virtual image with visible light in a time-multiplexed manner. We demonstrate our proof-of-concept system on a bench-top setup and assess the appearance and contrasts of the displayed image. We also suggest potential improvements for current prototypes to encourage the community to explore this occlusion approach.

Index Terms: Human-centered computing—Human computer interaction (HCI)—Interaction paradigms—Mixed / augmented reality; Human-centered computing—Communication hardware, interfaces and storage—Displays and imagers

*e-mail: ooic@tcd.ie
†e-mail: yhiroi@g.ecc.u-tokyo.ac.jp
‡e-mail: yuta.itoh@iii.u-tokyo.ac.jp

1 Introduction

Optical see-through near-eye displays (OST-NEDs) allow users to view virtual images overlaid on their field of view. OST-NEDs are expected to play an important role in augmented reality (AR) applications, which enhance the user's perception by adding virtual content to their see-through view of the real environment. In AR applications, it is often desirable for the displayed image to be indistinguishable from reality [14]. Perceptual realism, in which the visual characteristics of the displayed image resemble those of reality, affects the overall realism of the displayed image. In the case of ghosting effects, in which the virtual image appears as transparent or semi-transparent against the background, the perceptual realism of the virtual image is deteriorated.

To address ghosting effects, researchers have explored optical occlusion techniques, which create mutual occlusion between real and virtual objects [21]. To enable optical occlusion capabilities in OST-NEDs, it is necessary to spatially modulate light from reality. However, current methods for achieving this have several limitations, including the inherent difficulty in miniaturizing the optical system and the degradation of see-through visibility. In particular, the negative impact of transmissive or reflective spatial light modulators (SLMs), masks that are essential for optical occlusion, has been overlooked with regard to see-through visibility.Transmissive SLMs have the advantage of a thin form factor, however they also suffer from a degradation of see-through views due to the diffraction caused by the pixel electrodes, which is known as the screen-door effect (SDE). In contrast, reflective SLMs inevitably have a larger form factor due to the need for an optical system that reflects the light back to the eye.

Chae et al. proposed an occlusion-capable OST-NED with photochromic material to address the SDE in a transmissive occlusion mask [6]. This system produces an occlusion image by projecting spatially modulated UV light onto photochromic materials. The photochromic occlusion mask itself lacks an internal pixelated struc-

ture, thereby avoiding the SDE and enabling both occlusion and a clear see-through view. However, this system uses multiple SLMs and beam splitters to form an occlusion image with UV light and a virtual image with visible light, making it difficult to miniaturize the system for wearable devices.

This paper proposes a design for a photochromic occlusion-capable OST-NED that can be miniaturized in principle. Our design combines a single SLM, a photochromic plate, and a stack of transmissive and reflective holographic lenses (HOLs). These HOLs are designed to respond to different wavelengths of light. Specifically, the reflective HOL responds only to visible light and displays a visible virtual image to the viewpoint. In contrast, the transmissive HOL responds only to UV light and creates an occlusion mask on the photochromic plate. This design eliminates the SDE and enables a single SLM to control both the occlusion mask and the virtual image, resulting in a more compact occlusion-capable OST-NED without sacrificing the clarity of the see-through view.

Our main contributions include the following:

- Proposing a compact occlusion-capable OST-NED design that avoids the SDE by using a single SLM and photochromic plate.
- Demonstrating a proof-of-concept display built as a bench-top system.
- Outlining the limitations of the our prototype and exploring potential research directions for photochromic optical occlusion techniques with HOLs.

2 Related Work

In this section, we briefly review existing works on occlusion-capable NEDs and display designs with HOLs.

2.1 Occlusion-Capable NEDs

Realizing occlusion in OST-NEDs requires relay optics that guide incoming light to SLMs. A typical design uses a $4f$ system with an SLM placed at the intermediate focus plane to achieve hard-edge occlusion. For SLMs, early occlusion approaches employ transmissive LCDs [20, 22].

A transmissive LCD can also be placed directly behind the display screen. This leads to occlusion optics with a slim and wide field-of-view (FoV), but with soft-edge occlusion, which inevitably causes defocused masks [25, 26]. To address this defocus issue, Itoh et al. proposed a method that fuses scene images onto the mask edges through an OST-NED to compensate for the defocus artifact [13]. However, the soft-edge design has additional undesirable diffraction artifacts, due to the grid structures of the electrodes and blank spaces between the pixels. The Magic Leap 2, a recently released commercial OST-NED, employs a diamond-shaped pixel shape for the mask to reduce diffraction artifacts.

Alternatively, using reflective SLMs, such as liquid crystal on silicon (LCoS), as occlusion masks can remove diffraction artifacts [18, 29]. LCoS-based occlusion-capable OST-NEDs combine different optics, such as x-cube prisms [4], free-form lenses [8, 9], multiple focus-tunable lenses [27], and affordable lens components [30, 31]. However, when using reflective SLMs for occlusion masks, the light from the real world must be directed to an SLM through a mirror and redirected to the original optical path while handling the viewpoint shift [31]. Although polarizing beam splitters [16] and paired ellipsoidal mirrors [34] are often employed to fold back the optical path, these methods inevitably increase the form factor of the overall system.

To address the elimination of the SDE, Chae et al. designed an OST-NED using a transmissive photochromic material as an occlusion mask [6]. This system has a larger form factor due to the two SLMs that control UV and visible light sources separately.

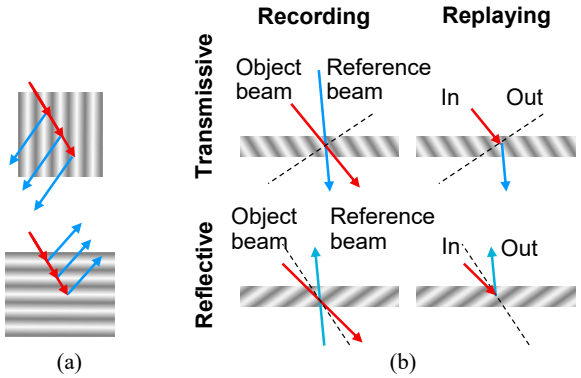

Figure 2: Illustrations of volume holograms. (a) Schematic diagrams of how volume holograms efficiently diffract a Bragg-angle incident light and create first-order diffracted light. (b) Schematic diagrams of hologram recordings and replays.

Unlike their work, we propose a compact, photochromic occlusion-capable OST-NED design that utilizes a single SLM to control both UV and visible light sources.

As an example of using a single SLM to control both occlusion and visible images, Krajancich et al. developed a system that switches between light from LEDs and that of the real world, using a single digital micromirror array (DMD) as a display screen [24]. This system has an inherently narrow FoV and difficulty avoiding viewpoint shift because the surface of the DMD is used as a display. In contrast, since we utilize a transmissive photochromic material for the occlusion mask, our system does not suffer from viewpoint shift and achieves a wide FoV.

2.2 HOLs for OST-NEDs

HOLs are optical elements based on the diffraction of light. Compared to conventional refractive lenses, HOLs have attractive characteristics for OST-NEDs [2, 7, 15, 17, 28], including a thin form factor and high light efficiency due to their ability to selectively transmit specific angles and wavelengths of light.

In analog holography, a hologram is recorded by capturing the interference pattern between a reference light beam and an object light beam that originates from real objects [23]. Holography often utilizes photopolymers as photosensitive materials. Specifically, a photopolymer that has a sufficient relative thickness for the wavelength of the input light is referred to as a volume hologram [19]. This particular photopolymer is capable of efficiently diffracting light (Fig. 2 a).

The manufacturing process for HOLs is typically similar to that of analog holography. HOLs can be fabricated using a controlled coherent light source as the object light that incidents on the photopolymer in conjunction with a reference light. When the incident light reaches the HOL from the direction of the object light, the diffraction pattern on the HOL causes the light to be reflected or transmitted in the direction of the applied reference light (Fig. 2 b). Throughout the process, although the specific characteristics inherent to diffractive optical systems are included, it is possible to obtain a thin optical element that exhibits the same characteristics as the optical system designed at the time of recording [33].

We used stacked HOLs that separate the UV optical path for the occlusion mask from the visible optical path for virtual image generation. This is done by utilizing the wavelength dependence of the HOL. We outline the specific manufacturing procedures for our custom HOLs in Sec. 4.2.

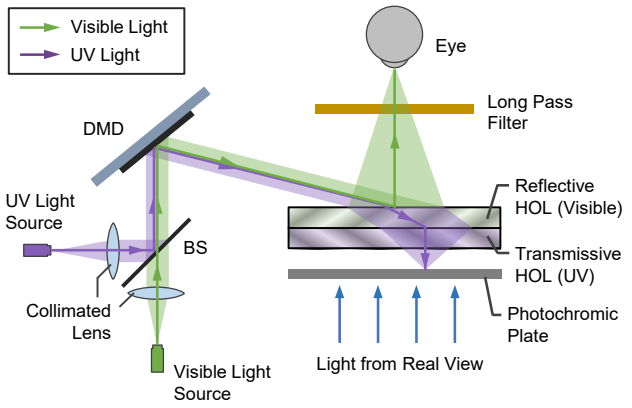

Figure 3: Schematic diagram of photochromic occlusion with stacked HOLs. The green arrows indicate the path of visible light, and the purple arrows indicate the path of UV light. The stacked holographic optical lenses (HOLs) differentiate the incident light by wavelength, with visible light being reflected back to the eye, and UV light being focused on the photochromic plate.

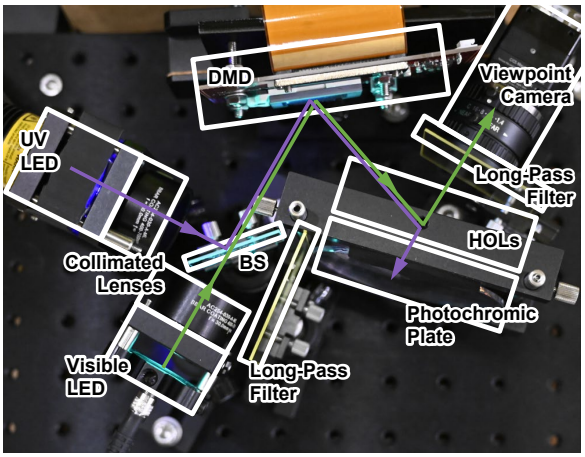

Figure 4: Hardware setup of our prototype. The schematic is identical to Fig. 3.

3 Photochromic Occlusion with Stacked HOLs

Figure 3 shows the schematic diagram of our prototype. Our system consists of UV and visible light sources, DMDs,photochromic plates, and stacked wavelength-dependent HOLs. The visible light source is employed to present virtual images to the eye, while the UV light source is used to illuminate photochromic plates to create occlusion masks. The visible and UV light sources are coaxially aligned by a beam splitter (BS) and incident on the DMD. The DMD is employed to form both the virtual image and the occlusion mask image. Since the horizontal orientation of the image differs between the virtual image and the occlusion mask, the image orientation on the DMD must be aligned for each light source. To achieve this, the DMD synchronously displays time-multiplexed images with different horizontal directions for each LED light source. We placed a long-pass filter in front of the eye to prevent undesirable UV light from entering the eye.

In the prototype, the stacked HOL plays a central role in forming visible and UV images in the user's field of vision and on the photochromic plate, respectively. The prototype uses two types of HOLs: reflective and transmissive. The reflective HOL responds to visible light, while the transmissive HOL responds to UV light. The reflective type is positioned so that the reflective type faces inward toward the user's eye, and the transmissive type faces outward toward the photochromic plate. More specifically, the reflective HOL is placed on the side of the eye, while the transmissive HOL is placed on the side of the photochromic plate. As a result, the reflective HOL enables visible light to be reflected to the observer. Furthermore, the UV light passing through the reflective HOL is focused by the transmissive HOL and forms an image on the photochromic plate.

4 Implementation

This section provides details on implementing a proof-of-concept system of our compact photochromic occlusion. First, we describe the hardware setup in Sec. 4.1, followed by an overview of the recording process for each of the HOLs in Sec. 4.2.

4.1 Hardware Setup

Figure 4 shows the actual setup of our prototype. In this prototype, we used a 0.9 mW, 405 nm LED (Thorlabs, PL205) as our UV light source and a 0.9 mW, 520 nm LED (Thorlabs, PL201) as our visible light source. For the DMD, we used a 0.65" DLP 6500 from Texas Instruments. For the photochromic plate, we extracted a photochromic lens from off-the-shelf sunglasses designed for emmetropic (0 diopters) eyes. The eyeglasses lens still had a small curvature, as shown in 1(a). However, we did not observe any impacting distortions in the image of the occlusion mask if we placed the lens close enough to the transmissive HOL. We also placed two long-pass filters (Thorlabs FGL420S) in the system to block unnecessary UV light.

4.2 HOL Recording

Figure 5 shows the recording setups of our transmissive and reflective HOLs, respectively. We used a 5 mW, 532 nm green laser from LitiHolo as our coherent light source in the HOLs recording process. As a photopolymer plate, we used Litiholo C-RT20 instant hologram film.

To record the transmissive HOL (Fig. 5 top), we set the photopolymer film perpendicular to the object beam while maintaining the incident beam at 0°. We split the reference beam from the object beam and collimated it. A plane mirror then reflected the collimated reference beam at 40° toward the photopolymer film. As a result, we produced a transmissive HOL with an angle of incidence of 40° and an angle of exit of 0°.

For this proof-of-concept study, we fabricated the HOL using photopolymers sensitive to the visible light band, which are readily available. In general, transmissive HOLs have a wide tolerance for the wavelength of the incident beam. Thus, transmissive HOLs can also diffract UV light, with some efficiency loss. If UV-sensitive photopolymers could be utilized instead [1], the photosensitive efficiency could be further enhanced, and the diffraction artifact of the scene light could be further minimized.

For the reflective HOL recording, we used a Denisyuk hologram setup, in which a beam with a single optical path serves as both object and reference light. A photopolymer film was positioned 40° away from the light source. When a concave mirror is placed behind the photopolymer, the light incident on the photopolymer becomes the object light, and the beam reflected by the concave mirror becomes the reference light. In our current prototype design, the concave mirror's angle was 10° away from the normal one of the photopolymer, which in this case was due to the constraints of the DMD and eye position. As a result, the HOL has an input angle of 40° and an output angle of 10°.

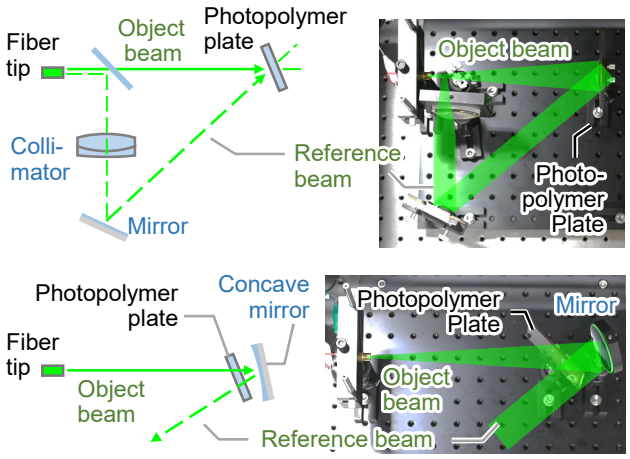

Figure 5: HOL recording setups. (top) A setup for a transmissive HOL and (bottom) for a reflective HOL.

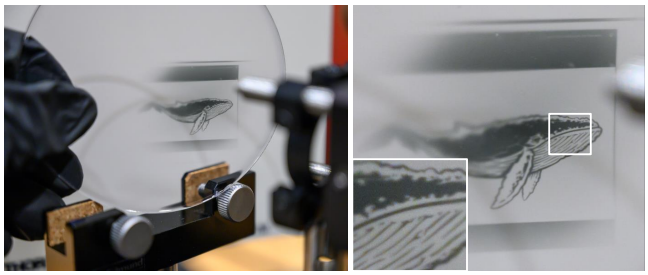

(a) (b)

Figure 6: A demonstration of photochromic occlusion using the UV light source, the DMD, and the projection lens. (a) When UV light is applied, an image is formed on the photochromic plate. (b) A close-up of the resulting occlusion mask. The material can produce a detailed image as a mask without the SDE.

5 Evaluation

In this section, we evaluate the performance of the implemented proof-of-concept prototype. First, prior to the use of the actual prototype, we verify the characteristics of the photochromic-based occlusion used in this study against an ideal setup. We then go on to evaluate the performance of the actual bench-top design.

5.1 Photochromic Occlusion

We first illustrate the efficacy of the photochromic occlusion mask through the utilization of an optimal configuration, comprising a UV light source, DMD, and a projection lens, and excluding the HOLs employed in our actual configuration. We used this configuration to assess the visibility of the mask image and the see-through view. We also evaluated the contrast response of the mask over time.

5.1.1 Mask and See-Through View Visibility

Figure 6 shows the outcome of displaying a mask image on the DMD and projecting the UV image onto the photochromic plate, where a mask image of a whale is discernible on the plate. As depicted in Fig. 6 (b), this plate can display a mask image without the SDE. In addition, the contrast degradation and diffraction artifacts are effectively removed in the see-through view.

5.1.2 Transmittance Ratio and Response Time

We then evaluated the transmittance ratio and response time of the photochromic plate with the aforementioned ideal configuration. We

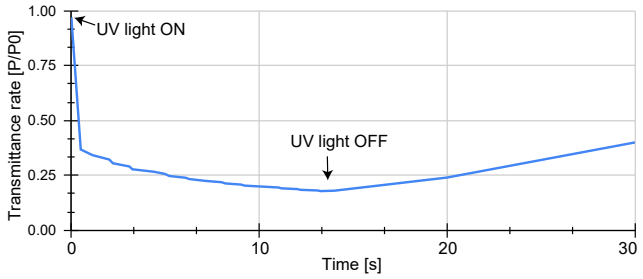

Figure 7: Transmittance rate of 516nm visible light according to the exposure time of the photochromic material under the 405nm UV light source.

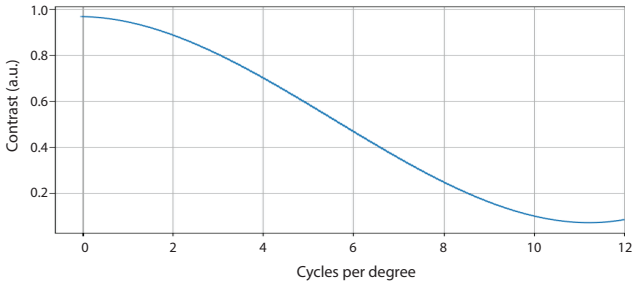

Figure 8: The MTF analysis of the virtual image.

used a 512 nm visible LED to measure transmittance. We calibrated the intensity of the visible LED when transmitted directly through the photochromic plate at 1, then we measured the intensity ratio of the visible LED that passed through the photochromic mask during UV illumination. First, we assessed the reaction time of the photochromic plate by exposing it to UV light. When the opacity reached its peak, we turned off the UV and timed the plate to return to its initial state.

As depicted in Fig. 7, when exposed to a UV light source, the transmittance ratio exhibited a precipitous decline to 0.32 at 400 ms, before reaching a peak of 0.20 at approximately 11 seconds. Upon termination of UV illumination at this peak, approximately 160 seconds was required for the transmittance ratio to return to its initial state. It should be noted that these values are contingent upon the photochromic material employed, and substitution with photochromic plates that exhibit a faster response (Sec. 6) is a viable option in principle.

5.2 Qualitative Analysis of the Prototype

To evaluate the performance of our prototype, we took images under different conditions: with and without a background, with and without the virtual image, and with and without the mask. In our current prototype, we manually controlled the UV and visible light images. We first turned on the UV light and displayed the mask image on the DMD, and then waited until the UV light activated the photochromic plate. At that point, we turned off the UV light and turned on the visible light while displaying the target image on the DMD. In the evaluation, we used a C-mount camera, Ximea MC031CG-SY-UB (2064×1544 pixels, color), and a C-mount lens from Computar Optics ($f = 8$ mm) as the viewpoint camera.

Figure 9 summarizes the results obtained from our bench-top prototype, demonstrating that our system can simultaneously display both the virtual image and the photochromic occlusion mask (Fig. 9 d). Note that the occlusion appears to have a soft edge, as our setup lacks the relay lens system typically used to create a hard-edge occlusion. The limitations of this design and potential solutions

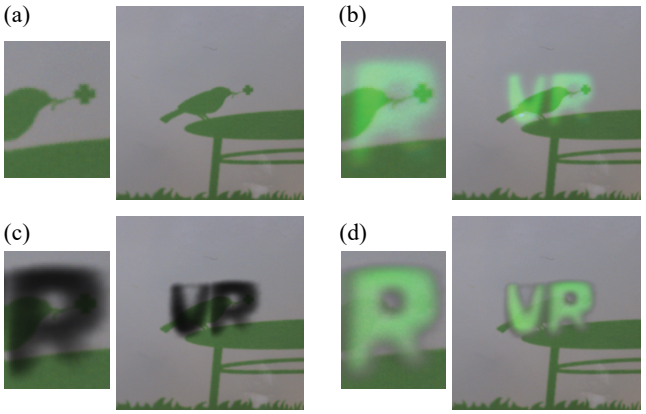

Figure 9: Qualitative evaluation of our system. We displayed virtual characters "VR" in the scene with our prototype with different display states. (a) The real scene. (b) Displaying the virtual characters without occlusion. (c) Displaying an occlusion mask only. (d) Displaying both the characters and the mask.

will be discussed further in the discussion section. Additionally, the density of the mask is limited by the maximum optical density achievable with the chosen photochromic material.

5.3 Resolution Analysis

To quantitatively evaluate the image quality of the current prototype, we investigated the resolution of the virtual image through slanted edge modulation transfer function (MTF) analysis [3]. Note that the MTF of the occlusion mask alone is not informative, since the current prototype configuration employs soft-edge occlusion, with the mask inserted directly in front of the eye. Therefore, the MTF of the virtual image with the mask displayed was measured instead.

We captured photographs of the test images as viewed through our prototype with an Ximea MC031CG-SY-UB camera equipped with a 16mm C-mount lens (Tamron M118FM16). Throughout the capture process, the F-number of the camera was set at 1.4. From the captured image, we extracted the regions of interest that contained slanted edges. The edge profiles from these regions of interest provided information about the variation from black to white pixels, including the spatial resolution of our prototype. Finally, we computed the MTF from the cropped region.

Figure 8 shows the MTF for the virtual image. The resolution of our system was 5.5 cycles per degree (cpd) with half contrast. Consumer-level near-eye displays typically offer resolutions of 5 to 15 cpd, and we confirm that our prototypes can present resolutions close to these displays. The current image quality degradation is largely due to hardware-dependent artifacts (Sec. 6). Therfore, improving the artifact will allow for higher resolution.

6 Discussion

The experiments showed that our prototype could simultaneously present both occlusion masks and virtual images through a single SLM while eliminating the SDE. However, our prototype still faces several challenges for practical implementation. This section discusses the remaining challenges and directions for further research.

Hardware-Dependent Artifacts While our prototype serves as a proof-of-concept, it is constrained by image quality limitations that primarily depend on the hardware currently in use. Specifically, the absence of a lens between the DMD and the HOLs in the current prototype results in diffuse reflection from the DMD, which leads to insufficient light reaching the HOLs, thus diminishing image quality. Additionally, using non-UV-sensitive photopolymers in the transmissive HOLs reduces the photosensitizing efficiency and increases the diffraction artifacts. Furthermore, the intensity of the laser light used to record the HOLs is weak, and the recording process was prolonged, which may have resulted in artifacts due to subtle vibrations and positional changes. To address these issues, the use of more powerful lasers ($\geq$ 500 mW) [17] would enable instantaneous recording of HOLs and minimize the artifacts.

Hard-Edge Occlusion The current prototype only achieves soft-edge, occlusion as the occlusion mask is positioned in close proximity to the eye, resulting in a blurred occlusion outline. To present hard-edge occlusion, it is necessary to focus the light from the scene through an occlusion mask. This is typically achieved through $4f$ optics [20, 31]. However, this approach tends to result in a bulky form factor.

Pancake optics [5, 32] would be a potential solution to achieve hard-edge occlusion. Traditional pancake optical systems integrate concave half mirrors, waveplates, and polarizers to expand the virtual optical path length. Recently, NEDs with pancake optical systems that use HOLs instead of concave half mirrors have been commercialized, such as Magic Leap 2. An avenue for future research is the integration of UV-sensitive HOLs into pancake optics that already employ visible HOLs, which would allow for thin, hard-edge occlusion-capable OST-NEDs to be developed.

Varifocal Occlusion Since our system is similar to how a projector projects images, a varifocal or multifocal virtual image can be achieved by incorporating a focus-tunable lens (FTL) between the DMD and the visible HOL. However, achieving a varifocal mask is more challenging, as the UV light from the DMD must always be focused on the photochromic plate. Thus, the photochromic plate must mechanically or optically change the depth in conjunction with the FTL. Since the photochromic plate is transmissive, recent work that achieves varifocal occlusion by mechanically [10] or optically [11] shifting a transmissive LCD may be referenced. Our approach, which can handle both virtual images and masks with a single SLM, would reduce the form factor of existing varifocal occlusion systems.

Temporal Response of Photochromic Plate Our prototype with conventional photochromic material cannot instantly display an occlusion mask due to the material's slow chemical reaction speed. Fortunately, photochromic chemistry has made significant progress in developing photochromic materials with rapid response times, with a half-life of 16 ms [12]. By incorporating these materials in photochromic plates, it is expected that the real-time presentation of occlusion masks will be feasible.

7 Conclusion

We proposed a compact, photochromic occlusion-capable near-eye display that utilizes layered HOLs and can handle both visible and UV light through a single DMD. This design provides a promising direction for developing compact occlusion-capable OST-NEDs with improved visibility. We demonstrated the capabilities of this system by implementing the proof-of-concept prototype and outlined its limitations and potential directions for future research.

Acknowledgments

This project was partially supported by JST FOREST Grant Number JPMJFR206E, and JSPS KAKENHI Grant Number JP20H04222, and JP20H05958, Japan, along with SFI D-REAL Grant No. 18/CRT/6224, Ireland.

References

[1] J. Aleksejeva and J. Teteris. Ultraviolet holographic recording in photopolymers. *physica status solidi (c)*, 8(9):2850–2853, 2011.

[2] T. Ando, T. Matsumoto, H. Takahasihi, and E. Shimizu. Head mounted display for mixed reality using holographic optical elements.

MEMOIRS-FACULTY OF ENGINEERING OSAKA CITY UNIVERSITY, 40:1–6, 1999.

[3] P. D. Burns et al. Slanted-edge mtf for digital camera and scanner analysis. In *Is and Ts Pics Conference*, pp. 135–138. Society for Imaging Science & Technology, 2000.

[4] O. Cakmakci, Y. Ha, and J. P. Rolland. A compact optical see-through head-worn display with occlusion support. In *Third IEEE and ACM ISMAR*, pp. 16–25. IEEE, 2004.

[5] O. Cakmakci, Y. Qin, P. Bosel, and G. Wetzstein. Holographic pancake optics for thin and lightweight optical see-through augmented reality. *Optics Express*, 29(22):35206–35215, 2021.

[6] M. Chae, K. Bang, Y. Jo, C. Yoo, and B. Lee. Occlusion-capable see-through display without the screen-door effect using a photochromic mask. *Optics Letters*, 46(18):4554–4557, 2021.

[7] C. Chang, K. Bang, G. Wetzstein, B. Lee, and L. Gao. Toward the next-generation vr/ar optics: a review of holographic near-eye displays from a human-centric perspective. *Optica*, 7(11):1563–1578, Nov 2020. doi: 10.1364/OPTICA.406004

[8] C. Gao, Y. Lin, and H. Hua. Occlusion capable optical see-through head-mounted display using freeform optics. In *11th IEEE ISMAR*, pp. 281–282, 2012.

[9] C. Gao, Y. Lin, and H. Hua. Optical see-through head-mounted display with occlusion capability. In *Proc. SPIE*, vol. 8735, pp. 87350F–1:9, 2013.

[10] T. Hamasaki and Y. Itoh. Varifocal occlusion for optical see-through head-mounted displays using a slide occlusion mask. *IEEE TVCG*, 25(5):1961–1969, 2019.

[11] Y. Hiroi, T. Kaminokado, S. Ono, and Y. Itoh. Focal surface occlusion. *Opt. Express*, 29(22):36581–36597, Oct 2021. doi: 10.1364/OE.440024

[12] N. Ishii, T. Kato, and J. Abe. A real-time dynamic holographic material using a fast photochromic molecule. *Scientific reports*, 2(1):1–5, 2012.

[13] Y. Itoh, T. Hamasaki, and M. Sugimoto. Occlusion leak compensation for optical see-through displays using a single-layer transmissive spatial light modulator. *IEEE TVCG*, 23(11):2463–2473, 2017.

[14] Y. Itoh, T. Langlotz, J. Sutton, and A. Plopski. Towards indistinguishable augmented reality: A survey on optical see-through head-mounted displays. *ACM Computing Surveys (CSUR)*, 54(6):1–36, 2021.

[15] C. Jang, K. Bang, S. Moon, J. Kim, S. Lee, and B. Lee. Retinal 3d: augmented reality near-eye display via pupil-tracked light field projection on retina. *ACM TOG*, 36(6):190:1–190:13, Nov. 2017. doi: 10.1145/3130800.3130889

[16] T. Kaminokado, Y. Hiroi, and Y. Itoh. Stainedview: Variable-intensity light-attenuation display with cascaded spatial color filtering for improved color fidelity. *IEEE TVCG*, 26(12):3576–3586, 2020. doi: 10.1109/TVCG.2020.3023569

[17] J. Kim, Y. Jeong, M. Stengel, K. Akşit, R. Albert, B. Boudaoud, T. Greer, J. Kim, W. Lopes, Z. Majercik, P. Shirley, J. Spjut, M. McGuire, and D. Luebke. Foveated ar: Dynamically-foveated augmented reality display. *ACM Trans. Graph.*, 38(4), July 2019. doi: 10.1145/3306346.3322987

[18] K. Kim., D. Heo., and J. Hahn. Occlusion-capable head-mounted display. In *Proceedings of the 7th International Conference on Photonics, Optics and Laser Technology - Volume 1: PHOTOPTICS,*, pp. 299–302. INSTICC, SciTePress, 2019. doi: 10.5220/0007612702990302

[19] N. Kim, Y.-L. Piao, and H.-Y. Wu. Holographic optical elements and application. *Holographic Materials and Optical Systems*, 5:99–131, 2017.

[20] K. Kiyokawa, M. Billinghurst, B. Campbell, and E. Woods. An occlusion-capable optical see-through head mount display for supporting co-located collaboration. In *2nd IEEE ISMAR*, p. 133, 2003.

[21] K. Kiyokawa, Y. Kurata, and H. Ohno. An optical see-through display for mutual occlusion of real and virtual environments. In *Augmented Reality, 2000.(ISAR 2000). Proceedings. IEEE and ACM International Symposium on*, pp. 60–67. IEEE, 2000.

[22] K. Kiyokawa, Y. Kurata, and H. Ohno. An optical see-through display for mutual occlusion with a real-time stereovision system. *CG*, 25(5):765–779, 2001.

[23] H. Kogelnik. Coupled wave theory for thick hologram gratings. *Bell System Technical Journal*, 48(9):2909–2947, 1969.

[24] B. Krajancich, N. Padmanaban, and G. Wetzstein. Factored occlusion: Single spatial light modulator occlusion-capable optical see-through augmented reality display. *IEEE TVCG*, 26(5):1871–1879, 2020.

[25] A. Maimone and H. Fuchs. Computational augmented reality eyeglasses. In *12th IEEE ISMAR*, pp. 29–38, 2013.

[26] A. Maimone, D. Lanman, K. Rathinavel, K. Keller, D. Luebke, and H. Fuchs. Pinlight displays: Wide field of view augmented reality eyeglasses using defocused point light sources. In *ACM SIGGRAPH 2014 Emerging Technologies*, SIGGRAPH '14. Association for Computing Machinery, New York, NY, USA, 2014. doi: 10.1145/2614066.2614080

[27] K. Rathinavel, G. Wetzstein, and H. Fuchs. Varifocal occlusion-capable optical see-through augmented reality display based on focus-tunable optics. *IEEE transactions on visualization and computer graphics*, 25(11):3125–3134, 2019.

[28] L. Shi, F.-C. Huang, W. Lopes, W. Matusik, and D. Luebke. Near-eye light field holographic rendering with spherical waves for wide field of view interactive 3d computer graphics. *ACM TOG*, 36(6):1–17, 2017.

[29] T. Uchida, K. Sato, and S. Inokuchi. An optical see-through mr display with digital micro-mirror device. *Trans. of the Virtual Reality Society of Japan*, 7(2), 2002.

[30] A. Wilson and H. Hua. Design and prototype of an augmented reality display with per-pixel mutual occlusion capability. *Opt. Express*, 25(24):30539–30549, 2017. doi: 10.1364/oe.25.030539

[31] A. Wilson and H. Hua. Design of a pupil-matched occlusion-capable optical see-through wearable display. *IEEE TVCG*, 28(12):4113–4126, 2022. doi: 10.1109/TVCG.2021.3076069

[32] J. Xiong and S.-T. Wu. Planar liquid crystal polarization optics for augmented reality and virtual reality: from fundamentals to applications. *ELight*, 1(1):1–20, 2021.

[33] J. Xiong, K. Yin, K. Li, and S.-T. Wu. Holographic optical elements for augmented reality: principles, present status, and future perspectives. *Advanced Photonics Research*, 2(1):2000049, 2021.

[34] Y. Zhang, X. Hu, K. Kiyokawa, N. Isoyama, H. Uchiyama, and H. Hua. Realizing mutual occlusion in a wide field-of-view for optical see-through augmented reality displays based on a paired-ellipsoidal-mirror structure. *Opt. Express*, 29(26):42751–42761, Dec 2021. doi: 10.1364/OE.444904